

Explicit Finite Element Analysis of Convective-Conductive Heat Transfer

H. Laval, S. Giuliani, J. Donea

*Commission of the European Communities,
J.R.C. Ispra Establishment, Applied Mechanics Division, I-21020 Ispra (Varese), Italy*

ABSTRACT

The present paper discusses an explicit finite element approach to problems in transient convective-conductive heat transfer in a fluid region. The governing equations are the incompressible Navier-Stokes equations coupled with the thermal energy equation. Plane and axisymmetric problems are considered in terms of the primitive variables: velocity, pressure and temperature.

The space discretization is based on 4-node or 9-node quadrilateral finite elements, while a finite difference method is used for time integration. Due to the complexity of the governing equations, an explicit time discretization method is chosen in connection with a diagonal mass representation.

To deal with the necessarily implicit incompressibility constraint and the associated pressure terms, a fractional-step method is developed for marching in time. In this way, the pressure field is fully decoupled from and solved alternatively with the momentum equations. A weak treatment of the prescribed tangential components of velocity is introduced in order to avoid the spurious phenomenon of checkerboard splitting of the discrete pressure field encountered in other studies.

To illustrate the proposed fractional-step method, numerical examples are presented in plane and axisymmetric configurations using both bilinear and biquadratic local approximations. The solutions obtained are found in good agreement with previously published results.

1. INTRODUCTION

The ability to solve complex convective-conductive heat transfer problems is of prime importance in the safety analysis of nuclear reactor components. For large-scale analyses and in particular for 3-D problems, the use of non-linearly implicit time-stepping algorithms for integration of the Navier-Stokes and thermal energy equations appears to be quite demanding from the point of view of computational effort and computer storage. We have therefore been attracted by the algorithmic simplicity of explicit methods and have developed a fractional-step method for time integration of the semi-discrete equations produced by a finite element semi-discretization of the Navier-Stokes and thermal energy equations. The scope of the fractional-step method is to isolate the necessarily implicit pressure contribution from the other forcing terms (diffusion, advection, buoyancy effects) in the momentum equations and thereby permit an explicit time integration based on a lumped-diagonal mass matrix.

The following section deals with the basic equations and their discretization in space by the finite element method. Section 3 presents the explicit finite difference time discretization method and the associated mass lumping process. Section 4 discusses the fractional-step method and the weak treatment of the prescribed tangential velocities. Finally, section 5 is devoted to the presentation of results for natural and forced convection problems.

2. SEMI-DISCRETE EQUATIONS

The governing equations for the laminar flow of a Newtonian and incompressible fluid within the Boussinesq approximation are:

$$\rho \left(\frac{\partial \underline{u}}{\partial t} + \underline{u} \cdot \underline{\nabla} \underline{u} \right) = - \rho \underline{g} \alpha (T - T_r) + \underline{\nabla} \cdot \underline{\underline{\sigma}} \quad (1)$$

with

$$\underline{\underline{\sigma}} = - p \underline{I} + 2\mu \underline{\underline{D}}(\underline{u}) \quad (2)$$

The incompressibility condition is enforced through the continuity equation

$$\underline{\nabla} \cdot \underline{u} = 0 \quad (3)$$

The transport of thermal energy in the fluid is described by

$$\rho C_p \left(\frac{\partial T}{\partial t} + \underline{u} \cdot \underline{\nabla} T \right) + \underline{\nabla} \cdot \underline{q} - Q = 0 \quad (4)$$

with

$$\underline{q} = - K \underline{\nabla} T \quad (5)$$

where t is the time, \underline{u} the velocity field, p the pressure (including the hydrostatic component), T the temperature, ρ the density, $\underline{\underline{\sigma}}$ the stress tensor, $\underline{\underline{D}}$ the deformation tensor, \underline{q} the heat flux, Q the volumetric heat source, μ the dynamic viscosity,

C_p the heat capacity, K the thermal conductivity, α the coefficient of volume expansion, T_r a reference temperature for which the buoyancy forces are zero, \underline{I} the identity tensor and \underline{g} the gravity acceleration vector.

Either the velocity components or the total surface stress (traction) are specified on the boundary. The thermal part requires a temperature, a heat flux or a convective heat transfer condition, to be specified on the boundary. Initial conditions are given for the velocity and the temperature.

A weak formulation of the equations (1) to (5) is easily obtained via the Galerkin method and the introduction of finite elements in space leads to the semi-discrete equations. Two different spatially discrete models are considered. Both models are based on Lagrangian quadrilateral finite elements and make use of interpolations of different order for the velocity and the pressure. Continuity of the pressure across interelement boundaries is not requested, while the interpolation of the velocity must have a C^0 -continuity. The first model is based on 4-node isoparametric elements with bilinear local velocity and temperature fields and elementwise constant pressure. The second model uses 9-node isoparametric elements with biquadratic local velocity and temperature fields and bilinear discontinuous pressure interpolation. The semi-discrete form of the problem (1) to (5) is written in matrix form /4, 14/ as:

$$[\underline{M}] \{\dot{\underline{u}}\} + [\underline{A}] \{\underline{u}\} + [\underline{K}] \{\underline{u}\} - [\underline{C}] \{p\} + [\underline{G}] \{T - T_r\} = \{\underline{F}\} \quad (6)$$

$$[\underline{C}]^T \{\underline{u}\} = \{0\} \quad (7)$$

$$[M] \{\dot{T}\} + [A] \{T\} + [K] \{T\} = \{F\}, \quad (8)$$

where $[M]$ is the mass matrix, $[A]$ the advection matrix, $[K]$ the diffusion matrix, $[C]$ the gradient matrix, $[G]$ the buoyancy matrix, $\{F\}$ provides the forcing function in terms of body and surface forces and $\{\underline{u}\}$, $\{T\}$ and $\{p\}$ are the vector of nodal values of velocity, temperature and pressure.

3. EXPLICIT TIME INTEGRATION

To arrive at a computationally simple and efficient method for solving the above non-linear equations, it is highly attractive to use an explicit finite difference time integration procedure. However, to make an explicit scheme viable, it is necessary to put the mass matrix $[M]$ into a diagonal form. For that purpose, let us write the time derivative term in the form:

$$[M] \{X\} = \left\{ \int_V N_i (\sum_j N_j \dot{X}_j) dV \right\}, \quad (9)$$

where X represents either the velocity vector \underline{u} or the temperature T , N denotes the shape function and i and j are nodal indices. We can develop expression (9) as follows:

$$\begin{aligned}
[M] \{ \dot{X} \} &= \left\{ \int_V N_i (N_i \dot{X}_i + \sum_{j \neq i} N_j \dot{X}_j) dV \right\} \\
&= \left\{ \int_V N_i \left((1 - \sum_{j \neq i} N_j) \dot{X}_i + \sum_{j \neq i} N_j \dot{X}_j \right) dV \right\} .
\end{aligned}$$

It follows that

$$[M] \{ \dot{X} \} = \left\{ \int_V N_i \dot{X}_i dV + \sum_j \int_V N_i N_j (\dot{X}_i - \dot{X}_j) dV \right\} \quad (10. a)$$

or

$$[M] \{ \dot{X} \} = [M_d] \{ \dot{X} \} + ([M] - [M_d]) \{ \dot{X} \} . \quad (10. b)$$

Equations (10) show that the "consistent" time derivative term consists of two parts. The first term in the right-hand side of (10. a) defines a diagonal mass matrix $[M_d]$ obtained by adding all terms of each row of the consistent mass matrix $[M]$ and placing the results on the diagonal. The second term in equations (10) may be seen as an implicit correction term which couples the nodal values of the time derivative term. This second term is usually neglected when a diagonal mass representation is desired. However, its role is quite important for an accurate treatment of convection dominated problems, in the sense that it significantly improves the phase-speed characteristics of the spatially discrete equations. As shown in /5, 6/, we may preserve the beneficial effects of this implicit correction term even in a purely explicit-diagonal formulation simply by transferring it to the right-hand side of the discrete momentum equations.

Mass-lumping gives rise to difficulties when 9-node quadrilateral elements are employed to model axisymmetric configurations. In fact, the lumped nodal masses are found to be zero on the axis of symmetry. A solution to this problem is to substitute the dynamical equation corresponding to a node on the axis by a coherent "boundary" condition /9/.

Concerning the discretization in time, two different explicit schemes are used: the two-level Euler scheme and the three-level Adams-Bashforth scheme. The effects of combined space and time discretizations on the damping and frequency responses have been studied in /6, 7/.

The drawback of an explicit scheme is the stability condition which imposes a limit to the time step size. The stability conditions for combined convection-diffusion are derived in /7/.

4. FRACTIONAL-STEP METHOD

To deal with the incompressibility constraint, a fractional-step method is developed. The scope of this method is to isolate the necessarily implicit pressure contribution from the other terms (viscosity, transport, buoyancy effects) in the momentum equations and thereby permit explicit time-integration of the coupled system (6) - (8).

The method, originally proposed by Chorin /2/ in a finite difference context, is based on an orthogonal decomposition theorem due to Ladyzhenskaya /12/. By virtue of

this theorem, the momentum equations and the incompressibility condition in the Navier-Stokes problem can be treated according to a procedure consisting of two distinct phases or fractional steps. First, an intermediate velocity field \underline{u}^* , not satisfying the incompressibility condition, is calculated as the solution of the momentum equations without the pressure term:

$$[\underline{M}] \left\{ \frac{\underline{u}^* - \underline{u}^{\text{old}}}{\Delta t} \right\} = \{ \underline{F}^{\text{old}} \} - [\underline{A}] \{ \underline{u}^{\text{old}} \} - [\underline{K}] \{ \underline{u}^{\text{old}} \} - [\underline{G}] \{ T^{\text{old}} - T_r \} . \quad (11)$$

The boundary conditions are applied to the intermediate velocity field. Note that other time integration schemes can be used in (11) instead of Euler's. The final velocity $\underline{u}^{\text{new}}$ is obtained by adding to \underline{u}^* the dynamical effect of the pressure p^{new} , determined so that the incompressibility condition remains satisfied. So the intermediate velocity is decomposed into a divergenceless field and a gradient vector field. The former is the final divergenceless velocity field, whereas the latter is related to the pressure gradient. As a result, only normal boundary conditions are applied to the final velocity field. This feature was pointed out by Chorin /3/. The second step reads:

$$[\underline{M}] \left\{ \frac{\underline{u}^{\text{new}} - \underline{u}^*}{\Delta t} \right\} = [\underline{C}] \{ p^{\text{new}} \} \quad (12)$$

$$[\underline{C}]^T \{ \underline{u}^{\text{new}} \} = \{ 0 \} . \quad (13)$$

It is important to notice how the boundary conditions on the velocity are imposed in the present fractional-step method. In the first step, all the components of the boundary velocity are imposed whereas, in the second step, only the normal component is imposed on the final velocity field. Consequently, the boundary conditions for the tangential components of the velocity will be satisfied in a weak sense only.

The matrices $[\underline{C}]$ and $[\underline{C}]^T$ are rectangular matrices and differ in that the degrees of freedom of the velocity corresponding to the component normal to the boundary are excluded in the construction of $[\underline{C}]$ whereas they are retained in $[\underline{C}]^T$. The equation (13) can be rewritten:

$$[\underline{C}]^T \{ \underline{u}^{\text{new}} \} = \{ B \} \quad (14)$$

where $\{ B \}$ includes the normal boundary conditions. The equations (12) and (14) represent a linear system of coupled equations for the unknowns $\underline{u}^{\text{new}}$ and p^{new} . The dimension of the system is equal to the number of the degrees of freedom of velocity and pressure altogether.

We showed in /7/ that the second step leads to a projection operation. In fact, equation (12) is solved with respect to $\underline{u}^{\text{new}}$:

$$\{ \underline{u}^{\text{new}} \} = \{ \underline{u}^* \} + \Delta t [\underline{M}]^{-1} [\underline{C}] \{ p^{\text{new}} \} . \quad (15)$$

Now, substituting $\underline{u}^{\text{new}}$ from (15) into (14), we obtain the following linear system which governs the pressure field:

$$[\underline{C}]^T [\underline{M}]^{-1} [\underline{C}] \{P^{\text{new}}\} = (\{B\} - [\underline{C}]^T \{\underline{u}^{\text{old}}\}) / \Delta t \quad (16)$$

The matrix of this system exhibits a rank deficiency in the case of purely Dirichlet boundary conditions which is in relation with the well-known fact that the pressure is defined up to an additive constant. The system (16) can be solved for p^{new} and $\underline{u}^{\text{new}}$ is found by (15).

It is found (see /4, 7, 13, 14/) that the relaxation of the prescribed tangential velocity condition is essential to avoid the phenomenon of checkerboard splitting of the pressure field encountered on square meshes of 4-node elements with elementwise constant pressure or 9-node elements with bilinear discontinuous pressures. This is an unavoidable consequence of the use of conforming finite elements in the solution of problems involving an incompressibility constraint /8/.

The velocity field being now determined, the temperature equation may be integrated. Using Euler's scheme we calculate

$$[M] \left\{ \frac{T^{\text{new}} - T^{\text{old}}}{\Delta t} \right\} = \{F^{\text{old}}\} - [A] \{T^{\text{old}}\} - [K] \{T^{\text{old}}\} \quad (17)$$

where T satisfies the boundary conditions.

The above computational scheme for problems in transient convective-conductive heat transfer leads to a very simple computer program architecture (see /4, 14/).

5. NUMERICAL EXAMPLES

A first example is the determination of buoyancy-driven flow and heat transfer in a square enclosed cavity. The vertical walls of the cavity are maintained at different temperatures and the horizontal walls are thermally insulated. A solution is sought for a Rayleigh number $Ra = 10^6$ and a Prandtl number $Pr = 0.71$ using a graded mesh of 16×16 four-node elements or 8×8 nine-node elements. A pressure datum $p = 0$ is prescribed at the bottom left-hand corner. The transient calculation is started from an initial situation of zero velocities and temperature and repeated until a steady-state regime is reached. Figures 1 and 2 show steady-state contour plots of temperature and pressure using both discretizations. The present results are found to be in very good agreement with those obtained in the literature.

The second example determines the isothermal axisymmetric flow through a sudden expansion. At the channel inlet, we assume fully developed Poiseuille flow with a Reynolds number $Re = 200$. At the outlet, we adopted boundary conditions of zero surface tractions. The flow region is discretized with 800 four-node elements and 200 nine-node elements as suggested by Hughes et al. /10/. Figures 3 show the streamlines and the presence of a recirculation region in the wider part of the channel is clearly apparent. The pressure

contours are given in figures 4; the weak treatment of the tangential velocities along the boundary produced an extremely regular pressure field.

As a last example, we consider natural convection in a cylinder containing a radioactive isotope, as described by Kee et al. /11/. Experimental data are available and consist of temperature measurements along the axis and the radius of the cylinder. The Prandtl number is 0.7 and the modified Grashof number $2.78 \cdot 10^6$. Figures 5 show the steady-state contour plots of temperature, stream function and pressure obtained on using biquadratic elements. Figure 6 shows the steady-state temperature profile along the cylinder axis, while the radial temperature profile at mid-height of the cylinder is depicted in figure 7. Our results are seen to be in quite good agreement with the experimental data and with the solution obtained by the finite difference computer code NACOTEC /1/.

REFERENCES

- /1/ L. Biasi, L. Castellano, "Sviluppo di modelli numerici nel campo del PAHR", MTC/SF6/78, Matec, Milano, 1978.
- /2/ A. J. Chorin, "Numerical Solution of the Navier-Stokes Equations", Math. Comp., 22, 745-762, 1968.
- /3/ A. J. Chorin, "On the Convergence of Discrete Approximations of the Navier-Stokes Equations", Math. Comp. 23, 341-353, 1969.
- /4/ J. Donea, S. Giuliani, "The computer Code CONDIF for Transient Convective-Conductive Heat Transfer", Commission of the European Communities, EUR 6822, 1980.
- /5/ J. Donea, S. Giuliani, "A Simple Method to Generate High-Order Accurate Convection Operators for Explicit Schemes Based on Linear Finite Elements", Int. J. Num. Methods in Fluids, Vol. 1, 1981.
- /6/ J. Donea, S. Giuliani, H. Laval, "Accurate Explicit Finite Element Schemes for Convective-Conductive Heat Transfer Problems", in Finite Element Methods for Convection Dominated Flows, T. J. R. Hughes Ed., AMD, 34, ASME, New York, 1979.
- /7/ J. Donea, S. Giuliani, H. Laval, L. Quartapelle, "Solution of the Unsteady Navier-Stokes Equations by a Finite Element Projection Method", Recent Advances in Numerical Methods in Fluids, Vol. 2, Pentech Press, 1981.
- /8/ J. Donea, S. Giuliani, K. Morgan, L. Quartapelle, Paper B7/6 SMIRT VI, Paris, 1981.
- /9/ J. P. Halleux, "Transient Non-Linear Finite Element Analysis of Axisymmetric Structures by Lumped-Explicit Methods", Paper M6/8, SMIRT VI, Paris, 1981.
- /10/ T. J. R. Hughes, W. K. Liu, A. Brooks, "Finite Element Analysis of Incompressible Viscous Flows by the Penalty Function Formulation", J. Comp. Phys., 30, 1-60, 1979.
- /11/ R. J. Kee, C. S. Landram, J. C. Miles, "Natural Convection of a Heat Generating

Fluid within Closed Vertical Cylinders and Spheres", Trans. ASME, Series C, 55, 1976.

- /12/ O.A. Ladyzhenskaya, "The Mathematical Theory of Viscous Incompressible Flow", 2nd Ed., Gordon and Breach, New York, 1969.
- /13/ H. Laval, "Etude Numérique des Courants de Convection par la Méthode des Eléments Finis", dissertation de doctorat, Louvain-La-Neuve, 1980.
- /14/ H. Laval, "CONVEC: A Computer Program for Transient Incompressible Fluid Flow Based on Quadratic Finite Elements", Commission of the European Communities, to be published.

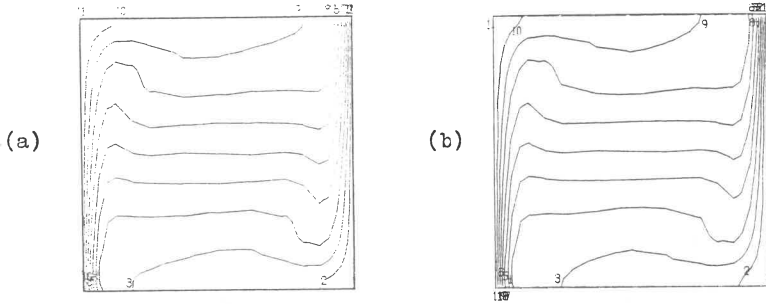


Fig. 1 : Temperature contours in thermal cavity : (a) 4-node, (b) 9-node

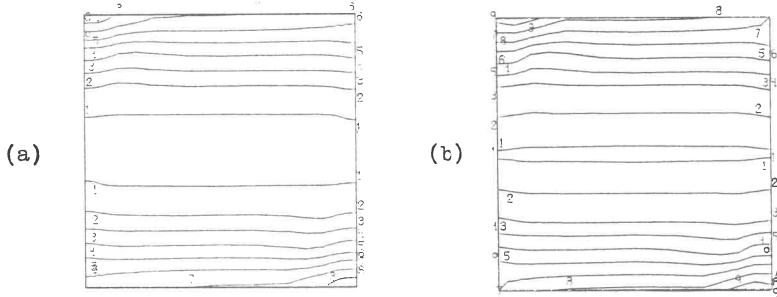


Fig. 2 : Pressure contours in thermal cavity : (a) 4-node, (b) 9-node.

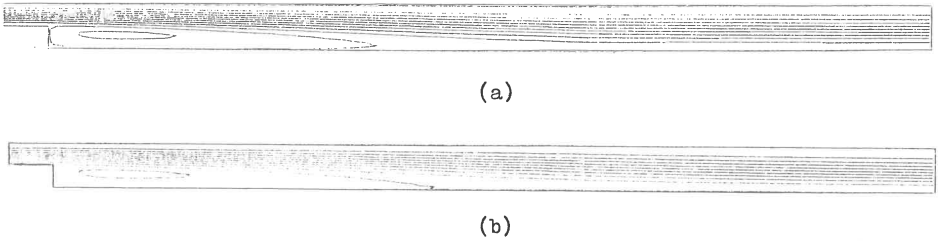


Fig. 3 : Axisymmetric flow through a sudden expansion ($Re=200$) : Streamlines ; (a) 4-node, (b) 9-node elements.

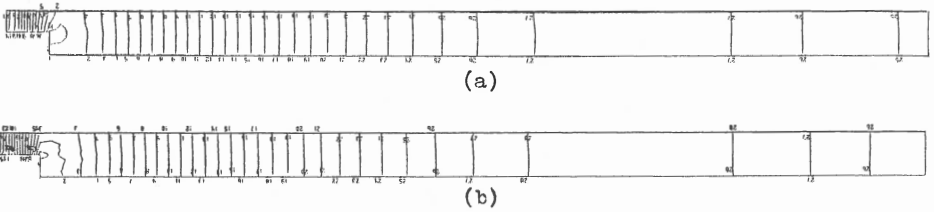


Fig. 4 : Flow through a sudden expansion ($Re=200$) : Pressure contours (a) 4-node, (b) 9-node elements.

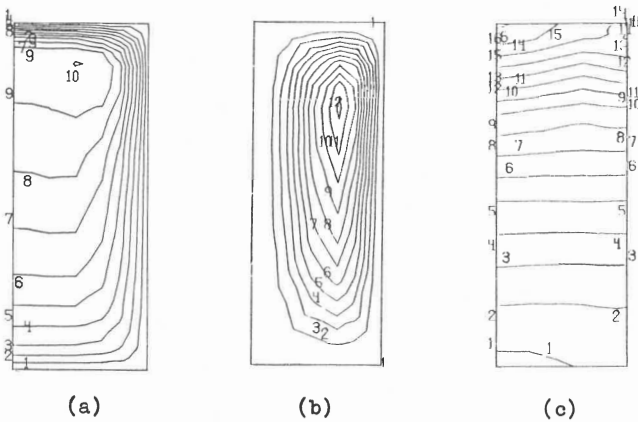


Fig. 5 : Natural convection in a heat generating cylinder ($Gr^* = 2.78 \cdot 10^6$) : (a) Temperature, (b) Stream function, (c) Pressure.

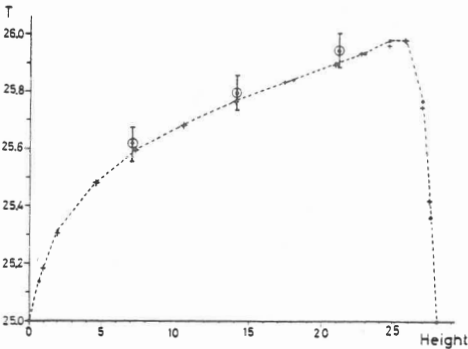


Fig. 6 : Natural convection in a heat generating cylinder : Temperature profile along cylinder axis. (•• 4-node, + 9-node elements, ⊕ experimental results /11/).

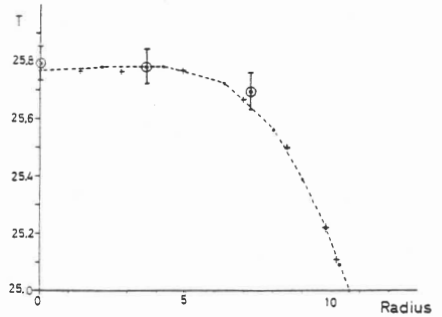


Fig. 7 : Natural convection in a heat generating cylinder : Radial temperature profile at mid-height of cylinder (same symbols as in Fig. 6).